ORIGINAL PAPER

Contribution of semiquantitative analysis with dynamic contrast enhanced magnetic resonance imaging to the differential diagnosis of focal liver lesions

Hanife Gülden Düzkalır [1], Naciye Kış [2], Deniz Akay Urgun [3],
Mehmet Oğuzhan Ağaçlı [4], Zeynep Gamze Kılıçoğlu [5]

[1] Kartal Dr. Lutfi Kirdar City Hospital, Department of Radiology, Istanbul, Turkey
[2] Department of Radiology, University of Medical Sciences, Prof Dr Cemil Tascıoglu City Hospital, İstanbul, Turkey
[3] Department of Radiology, University of California, USA
[4] Department of Radiology, University of Medical Sciences, Umraniye Education and Research Hospital, İstanbul, Turkey
[5] Department of Radiology, University of Medical Sciences, Haydarpaşa Education and Research Hospital, İstanbul, Turkey

ABSTRACT

Introduction and aim. We aimed to evaluate the usefulness of dynamic contrast-enhanced (DCE) MRI semiquantitative analysis values in focal liver lesions (FLL) to provide additional qualities that can be used in daily practice in the differential diagnosis of lesions.

Material and methods. This retrospective study included 91 patients with liver masses on DCE-MRI. The sensitivity and specificity of time intensity curves (TIC) and semiquantitative analysis values were evaluated to differentiate benign and malignant lesions.

Results. The study included 91 patients (376 lesions), aged between 28-81 years. Of the lesions, 303 were malignant and 73 were benign. In TIC semiquantitative analysis, it was found that "Tpeak" and "wash-out" rate values showed differences, especially in the differentiation of HCC, metastasis, and hemangioma. Area under curve, maximum relative enhancement, and "wash-in" and "wash-out" values of metastases and hemangiomas were different. Brevity of enhancement values of HSK, hemangiomas, and metastases were found to be different. The risk of malignancy was found to be high when the "wash-out" ratio was above 0.08 (sensitivity: 64.3%, specificity: 70.4%).

Conclusion. We think that the 0.08 threshold value we found for the washout ratio with DCE-MRI semiquantitative analysis data will be useful in daily practice in the differentiation of malignant and benign FLL.

Keywords. adult liver cancer, benign hepatoma, perfusion imaging

Introduction

Focal lesions of the liver (FLL) include epithelial, mesenchymal, mixed group primary benign or malignant tumors and secondary lesions. Common lesions with clinical significance include hemangioma, hepatic adenoma (HA), focal nodular hyperplasia (FNH), hepatocellular carcinoma (HCC), intrahepatic cholangiocellular carcinoma (IHCCC), and metastases.[1-4]

Magnetic resonance (MR) perfusion imaging is a quantitative technique that provides information about tissue microcirculation at levels below the spatial resolution of conventional imaging techniques.[5]

Corresponding author: Hanife Gülden Düzkalır, e-mail: hanifeduzkalir@gmail.com

Dynamic contrast-enhanced magnetic resonance imaging (DCE-MRI), which requires intravenous administration of gadolinium contrast, is often used to study FLL because it gives information about things like the growth of blood vessels in the tumor, its stage, its ability to spread to other parts of the body, and how it reacts to anti-tumor therapy.[1,6] Peak arterial contrast enhancement analysis is required to determine the intrinsic tissue properties of lesions and to detect neovascularization in its early stages.[7] The methods that can be used in the analysis of this contrast enhancement are grouped as: visual assessment, which may be subjective; semi-quantitative analysis obtained from time-intensity curves (TIC), which are automatically measured with the post-processing technique in the available software and measure the changes in contrast concentrations over time; and quantitative analysis, which requires highly complex formulas and a lot of time.[8] Therefore, we used a semiquantitative analysis technique in our study.

Aim

The aim of our study was to evaluate the usefulness of semi-quantitative analysis of abdominal DCE-MRI images in patients with diffuse malignant or benign FLL in providing additional features that can be easily used in daily practice to differentiate between lesions.

Material and methods

Ethical approval

This study does not contain any studies with human participants or animals performed by any of the authors. All data was processed anonymously, according to the privacy legislation.

Study design and study population

This study was carried out as a retrospective observational cross-sectional study at a single center. Patients aged between 18 and 85 years who underwent abdominal DCE-MRI in our clinic and who were found to have local liver lesions were retrospectively evaluated, and those who fulfilled the inclusion criteria were included in the study. Inclusion criteria:

– to have a primary or metastatic, benign or cancerous, focal lesion confirmed by imaging and/or clinical diagnostic criteria and histopathology;
– there are no MR contraindications (renal failure, respiratory failure, allergy, claustrophobia, and so on);
– to have optimum image quality for measurements.

Patients with an impaired general condition, an inability to establish respiratory cooperation, or an inappropriate condition for MRI (MR-incompatible prostheses, a cardiac pacemaker, etc.), those with artefactual images and masses smaller than 1 cm, were excluded from the study because optimal measurement could not be performed. A total of 376 (n) liver masses in 91 patients (F=41, M=50) (aged between 28 and 81) were included in the study. In patients with multiple lesions, lesions over 1 cm were included in the study. The hemangiomas included in the study (n=60) were diagnosed with MR appearance features and typical contrast enhancement patterns. Thirty-three of these lesions were already followed up with radiological imaging methods (ultrasound, computerized tomography, or MR).

Of the 203 metastatic masses in the study, 102 of these lesions were diagnosed as metastases in patients with known pathological diagnoses of primary malignancies (breast cancer, gastrointestinal tract, pancreas, etc.) during routine follow-up. The remaining 101 metastatic liver masses were biopsy-diagnosed lesions. Of the four adenoma patients included in the study as primary liver tumors, one had typical radiological imaging features; two were further confirmed by dynamic contrast-enhanced MRI with a liver-specific contrast agent; and one was definitively diagnosed by biopsy.

Among the patients included in the study, there was one case of focal nodular hyperplasia (FNH) and one case of malignant hemangioendothelioma diagnosed by imaging methods and biopsy. One patient was being followed up for an angiomyolipoma (AML). FNH and AML were excluded from the evaluation since they were numerically insufficient.

In 13 of our 15 hepatocellular carcinoma (HCC) cases, the radiological (American Liver Association; AASLD) and laboratory diagnostic criteria available in the literature were taken as references.[8] Histopathological diagnosis was available in two HCC cases. Ten of the HCC cases were followed up because of cirrhosis, seven because of chronic HBV, and four because of chronic HCV. Masses evaluated as dysplastic or regenerative nodules according to MR signal characteristics were not included in the study. One of the patients with IHCCC (n=2) was diagnosed histopathologically, and the other was diagnosed with typical radiological imaging features and clinical findings.

There was no diagnostic change in the clinical and radiological follow-up of all patients.

MRI techniques

Patients were asked not to take food for at least two hours before the examination, technical information was given, and informed consent was obtained. Subsequently, an IV cannula was inserted into one of the antecubital veins. All patients underwent routine upper abdominal dynamic contrast-enhanced MR examinations on a 1.5 Tesla MR machine (Philips Achieva) with a phased-array coil. In all cases, FOV was placed and a slice plan was applied to visualize the whole liver in the axial plane, and the liver was centralized to

reduce artifacts in the dome. Imaging included these sequences:

- T2-weighted axial plane turbo spin eko (TSE) with fat suppression (TR/TE: 386/80; tilt angle: 90°; slice thickness: 7.5 mm; FOV: 375),
- TSE T2 weighted (TR/TE: 524/80), TSE long TE T2 weighted (TR/TE: 520/200),
- T1 weighted gradient echo (TR/TE: 181/4.6 (in phase), 181/2.3 (out of phase), flip angle: 80°).
- Diffusion-weighted imaging (TR/TE: 1666/76; flip angle: 90°; slice thickness: 7.5 mm; slice spacing: 1.5 mm; FOV (field of view): average 375; matrix: 152x124) (single-shot echo-planar sequence, b=0 and b=1000 mm²/s),
- T1-weighted fat-suppressed dynamic contrast gradient echo (TR/TE: 4.1/1.9, flip angle: 10°, FOV: average 400, matrix: 196x224, slice thickness: 4 mm, slice spacing: 2 mm). The dynamic series were taken in five phases to avoid missing the arterial phase due to possible technical problems.

After the contrast-enhanced exam, all of the patients were kept under observation for about 45 minutes. If there were no problems, the patients were sent home.

MRI analysis techniques

Using the quantitative analysis measurement in the software on the workstation, TIC curves were automatically made from DCE cross-sectional images, and semiquantitative analysis values for all lesions were taken from this screen (Fig. 1). All images were measured by a single radiologist with at least 3 years of abdominal radiology experience.
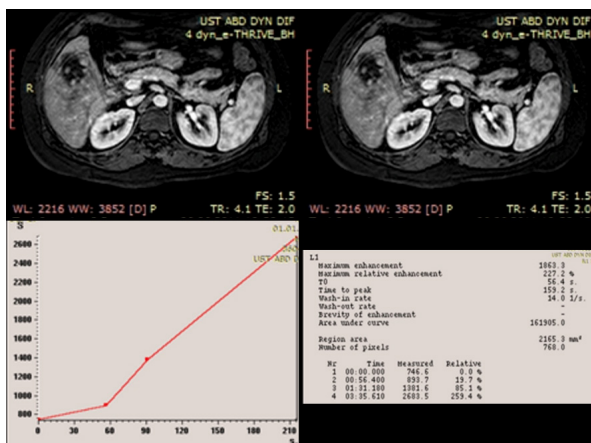

Fig. 1. Hemangioma (in a 39-year-old woman): Early arterial and late phase images of the lesion in dynamic series and semiquantitative analysis values with TIC

In the measurements, if the lesion had a homogeneous internal structure and was round in shape, the region of interest (ROI) was placed in a way to include the entire lesion without extending beyond the mass (Fig. 2). In non-round homogenous lesions, the borders of the mass were drawn with a "free-hand" ROI. For lesions below 2.5 cm, the ROI was measured to cover the entire lesion. For lesions of 2.5 cm or more and lesions with heterogeneous internal structure, measurements were made both by placing an ROI covering the entire lesion and by placing an ROI on the solid peripheral part of the lesion that retains the most contrast (Fig. 3). The average of three measurements from the same section was taken in large lesions.
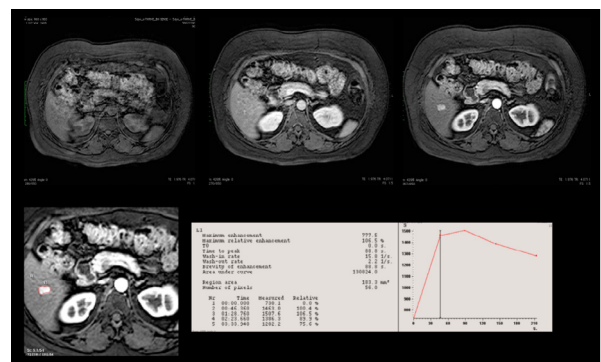
Fig. 2. Adenoma: (46 years old, female) A-TSE T2A, B- DWI b 1000, C, D, E- Time-intensity curve and semiquantitative analysis values of the lesion in the arterial phase and the whole lesion in the dynamic series
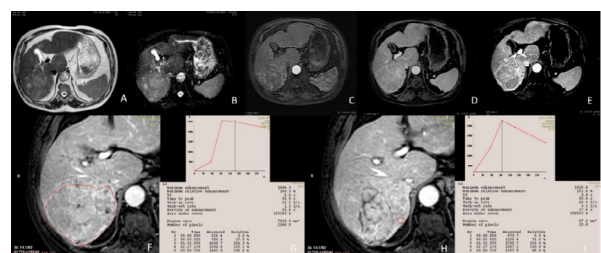
Fig. 3. Hepatocellular carcinoma: (62 years-male) A-TSE T2A, B- DWI b 1000, C, D, E- Lesion in dynamic series, F, G- Time-intensity curve and semiquantitative analysis values of the whole lesion in arterial phase in dynamic series, H, I- Time-intensity curve and semiquantitative analysis values of the partial lesion in dynamic series

In order to compare the lesion values, measurements were made from the right lobe posterior segment of normal liver tissue in each patient, with 1-cm-diameter ROIs placed in 3 different localizations in each section and averaged. In patients who could not be measured due to massive lesions in the right lobe posterior, measurements were made from other segments of the right lobe or the left lobe, which were at least 2 cm away from the lesions and did not contain vascular structures. Automatically obtained TIC curves were grouped as type 1, type 2, and type 3 patterns (Figure 4).
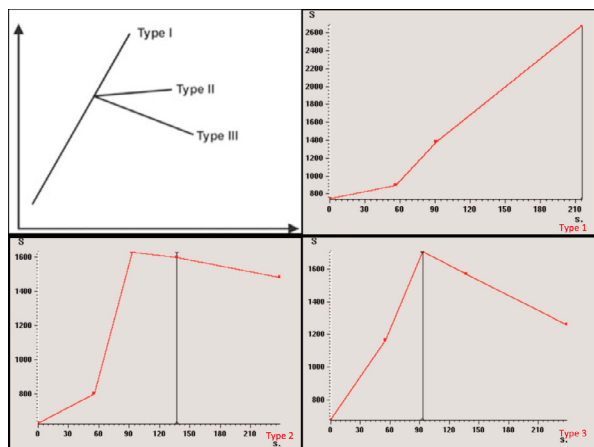
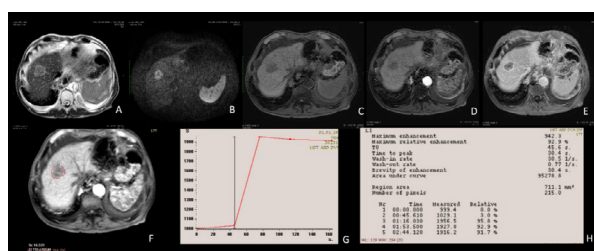**Fig. 4.** Types of TIC curves

Fig. 5. TIC curve: maximum intensity (1), maximum contrast enhancement (2), time to peak (3), wash-in (4) and wash-out (5) rates, and brevity of enhancement (6)

The following parameters were obtained from the TIC curve (Fig. 5):
– T0: the moment of contrast arrival in the tissue.
– S0: intensity before contrast arrival
– Maximum Intensity: The peak value of the curve
– Maximum contrast enhancement: the difference between the peak value and S0
– Time to peak (uptake rate) (TTP): the time difference between T0 and the time of peak intensity
– "Wash-in rate (staining rate): The tangent of maximum tangency between T0 and peak intensity time. It indicates the maximum rate of contrast medium uptake. This allows the early, strong contrast uptake of tumor tissue to be adequately estimated.
– "Wash-out" rate: the tangent of maximum steepness between the time of peak intensity and the last measurement point It indicates the maximum clearance rate of the contrast medium.
– "Brevity of enhancement" (BOE): The time between "wash-in" and "wash-out."
– Relative contrast enhancement (RCE): the percentage of signal intensity that increases between post-contrast and pre-contrast signal intensities, respectively.
– Maximum relative contrast enhancement (MRE): percentage of the signal intensity increase between

the maximum post-contrast and pre-contrast signal intensities.
– The area under the curve (AUC): the integral of the curve divided by the area under the TIC.

Statistical analysis

Statistical analyses were performed using MedCalc for Windows (MedCalc Software, Ostend, Belgium). Statistical differences in TIC data were evaluated by an ANOVA test, and differences between groups were evaluated by the Student-Newman-Keuls test. Frequency and the chi-square test were used to compare the morphological characteristics of the lesions in the T_1 and T_2 weighted series. The receiver operating characteristic (ROC) curve method was used to determine the "cut-off" (threshold value) for the benign-malignant differentiation of the lesion groups. The statistical significance level was set at $p<0.05$.

Results

Patient data

The number of patients in our study was 91 (M: 50 (54.9%); F: 41 (45.1%)). The age distribution was 28–81 years; the mean age was 55±15.7 years.

The total number of liver lesions evaluated was 376. Lesion sizes were 1–12.5 cm (mean 2.7 cm). 81% (n=303) of the lesions were malignant, and 19% (n=73) were benign.

The lesions included hemangiomas, HCC, metastases, adenomas, hemangioendothelioma, FNH, angiomyolipoma, and lymphoma. The distribution of the lesions is shown in Graph 1.
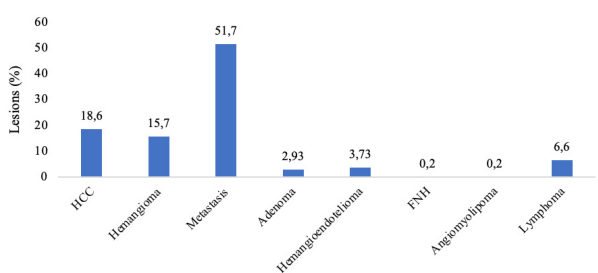

Graph 1. Distribution of lesions according to their types

Primary benign lesions (20%) were hemangiomas (n=60), adenomas (n=11), FNH (n=1), and AML (n=1). Primary malignant lesions included HCC (n=70), IHCCC (n=11), and malignant epitheloid hemangioendothelioma (n=14). Metastases (n=208) were predominantly gastrointestinal, including colorectal, gastric, esophageal, neuroendocrine carcinoma, gastrointestinal stomal tumor, gynecologic, prostate, pancreatic, and breast cancer (Fig. 6 and 7). The primary and metastatic distributions of the lesions are shown in Graph 2.
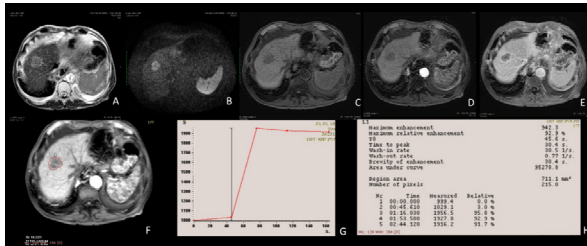
Fig. 6. Metastasis (stomach metastasis): (68 years old- male) A-TSE T2A, B- DWI b 1000, C, D, E- lesion in dynamic series, F, G, H- lesion in arterial phase in dynamic series, time-intensity curve and semiquantitative analysis values of the whole lesion
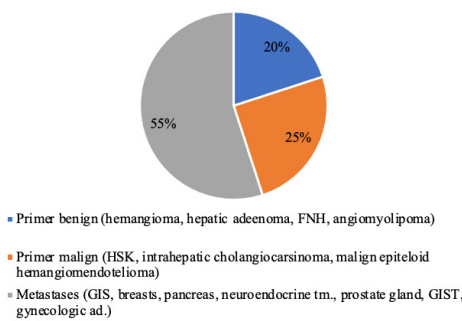
**Graph 2.** Distribution of primary and metastatic lesions

TIC semiquantitative analysis

The data for the TIC curves of the lesions are given in Table 1.

A paired comparison of AUC, MRE (F ratio: 3.602, p=0.001), and "wash-in" and "wash-out" (F ratio: 6.85, p<0.001) values of metastases and hemangiomas showed differences. Maximum enhancement and MRE values are different between hemangioendotheliomas and other groups (Graph 3). The wash-in rate of HCC was faster than metastases and hemangiomas (F ratio: 6.26, p<0.001). Metastases washed in more slowly than hemangiomas (Graph 4). There was a difference in TTP values in HCC, metastasis, and hemangiomas (p<0.001, F ratio: 11.63) (Graph 5).

The brevity of enhancement values were significantly different in HCC, hemangiomas, and metastases (F ratio: 3.51, p=0.001) (Table 2). The "wash in rate/wash out rate" value was higher in hemangiomas compared to metastases and HCC (F ratio: 2.43, P<0.02) (Graph 6). HCC washes out faster than metastases and hemangiomas (Graph 7).

In the ROC curve analysis used to determine the effectiveness of the "wash-out rate" value in the benign-malignant discrimination of lesion groups, the threshold value was found to be 0.08 (p<0.0001, 95% confidence interval: 0.61%–0.71%). At this cut-off value,
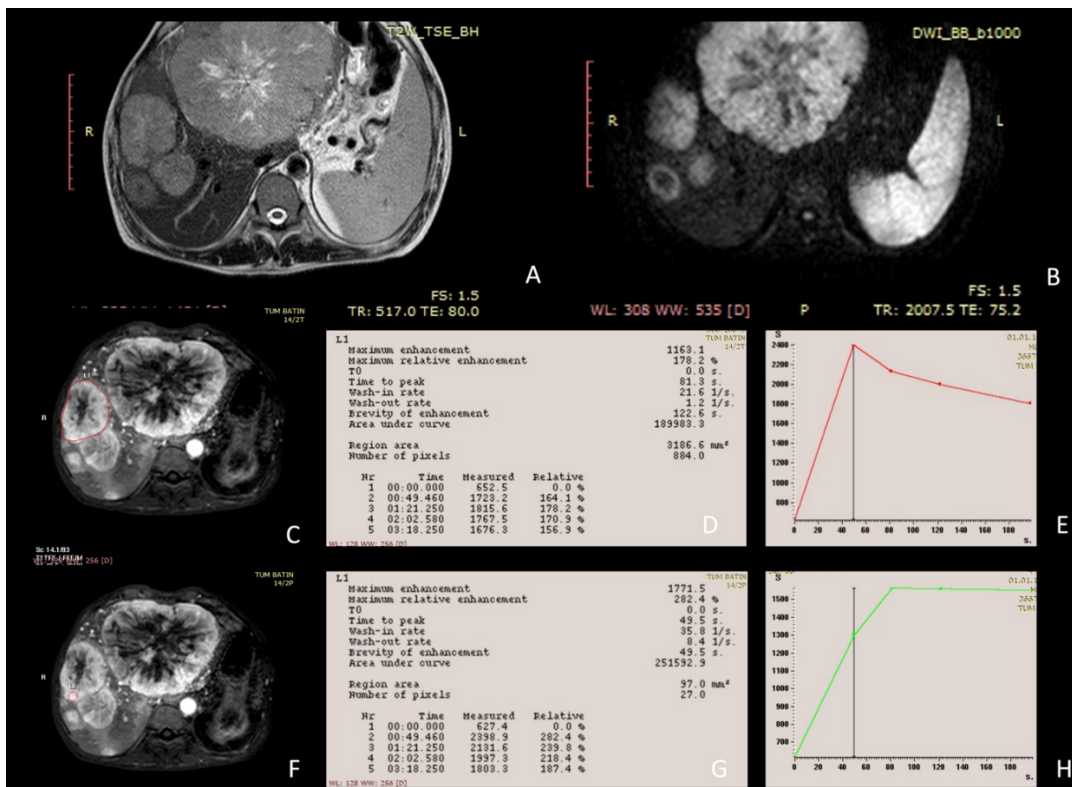

Fig. 7. Metastasis (neuroendocrine tumor): (41 years-male) A- TSE T2A, B- DWI b 1000, C, D, E- lesion in arterial phase in dynamic series, time-intensity curve and semiquantitative analysis values of the whole lesion, F, G, H- lesion in arterial phase in dynamic series, time-intensity curve and semiquantitative analysis values of the partial lesion

**Table 1.** Distribution of TIC data of the lesions

TIC MEAN/LESİONS	Hepatocelluler carcinoma	Metastase	Hemangioma	FNH	Hepatocelluler adenoma	Angiomyolipoma	Hemangioendotelioma	Lymphoma
AUC	176586.29	172292.02	130598.98	100745.	250616.27	191545	45594.14	101438.96
Brevity of enhancement	74.25	39.36	15.21	41.5	50.86	80.1	10.91	25.51
Maximum enhancement	1133.38	1053.09	989.01	489	1160.69	1024	199.52	827.47
Maximum rolative enhancement	137.8	126.2	156.09	57	138.64	87.3	64.32	132.81
T0	8.53	17.74	25.81	0	16.69	46.9	13.64	21.48
Tpeak	93.92	128.31	167.83	93.5	90.28	80.1	222.77	173.26
Wash in rate	19	19.07	15.33	7.4	20.96	20.9	4.03	10.66
Wash out rate	3.59	1.38	0.68	1	3.53	1.9	0.11	1.89
Wash in /wash out rate	10.01	23.47	69.99	7.4	8.34	11	28.56	20.24
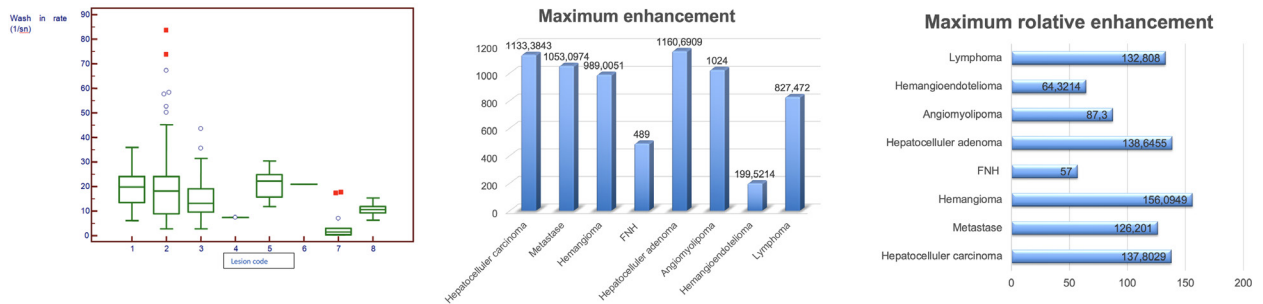
Graph 3. Distribution of the ME and MRE values of the lesions (1 = HCC, 2 = Metastasis, 3 = Hemangioma, 4 = FNH, 5 = Adenoma, 6 = Angiomyolipoma, 7 = Hemangioendothelioma, 8 = Lymphoma)
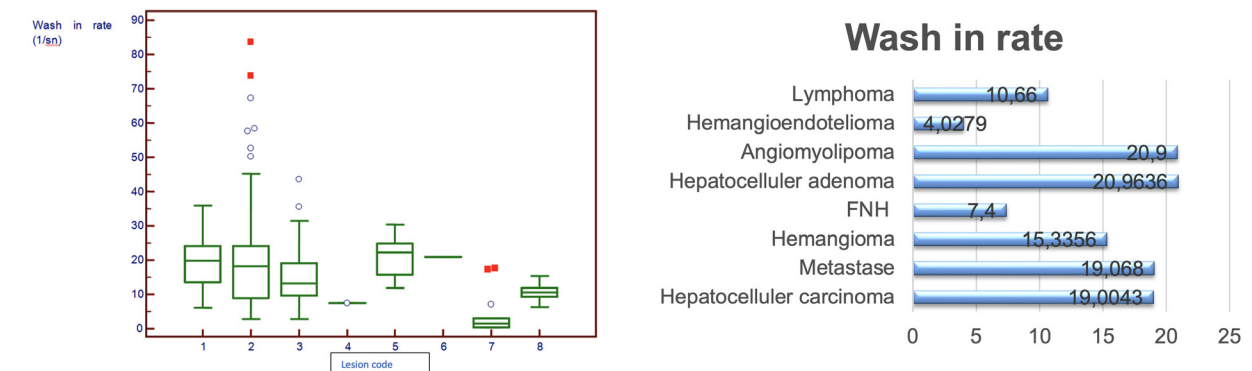
Graph 4. The distribution of the "wash-in" rates of the lesions (1 = HCC, 2 = Metastasis, 3 = Hemangioma, 4 = FNH, 5 = Adenoma, 6 = Angiomyolipoma, 7 = Hemangioendothelioma, 8 = Lymphoma)
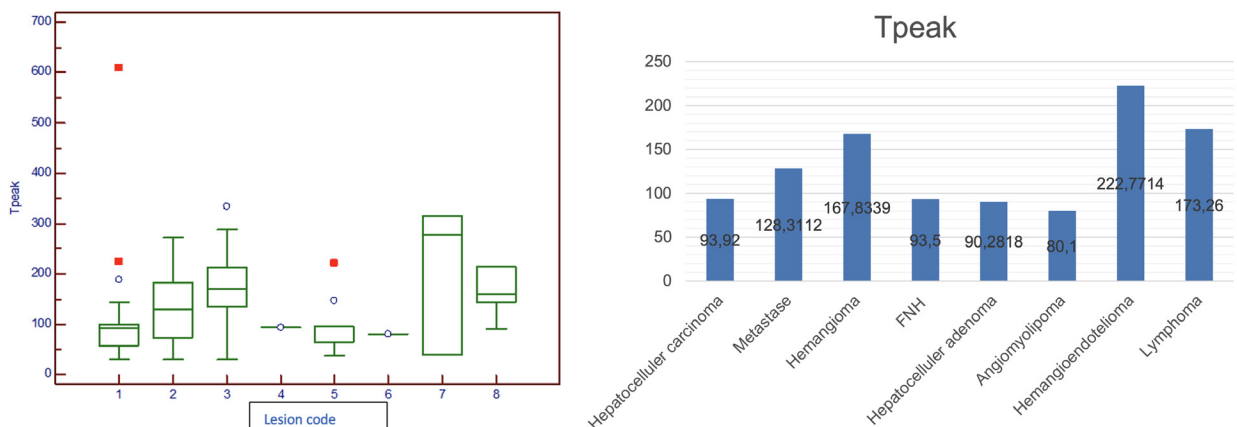
Graph 5. Distribution of the TTP values of the lesions (1 = HCC, 2 = Metastasis, 3 = Hemangioma, 4 = FNH, 5 = Adenoma, 6 = Angiomyolipoma, 7 = Hemangioendothelioma, 8 = Lymphoma)

Graph 6. Distribution of "Wash in rate"/"Wash out rate" values of the lesions (1 = HCC, 2 = Metastasis, 3 = Hemangioma, 4 = FNH, 5 = Adenoma, 6 = Angiomyolipoma, 7 = Hemangioendothelioma, 8 = Lymphoma)
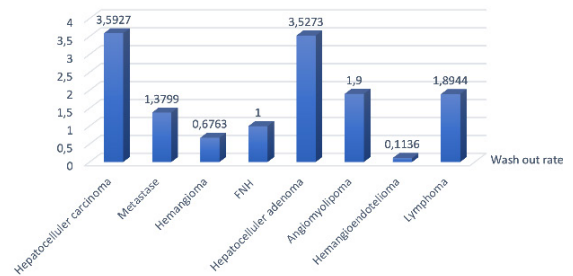
Graph 7. The distribution of the "Wash Out Rate" values of the lesions (1 = HCC, 2 = Metastasis, 3 = Hemangioma, 4 = FNH, 5 = Adenoma, 6 = Angiomyolipoma, 7 = Hemangioendothelioma, 8 = Lymphoma)

sensitivity was 64.3% (95% confidence interval: 58.3%–70.2%) and specificity was 70.4% (95% confidence interval: 58.4%–80.7%). The positive LR (likelihood ratio) was 2.18, and the negative LR was 0.51 (Graph 8).

Table 2. A comparison of the BOE values of the lesions (1 = hepatocellular carcinoma, 2 = metastasis, 3 = hemangioma, 4 = FNH, 5 = hepatocellular adenoma, 6 = angiomyolipoma, 7 = hemangioendothelioma, 8 = lymphoma)

Lesions	n	Mean	Different (p<0.05) from factor
(1)1	70	74.25	(2)(3)(7)(8)
(2)2	194	39.36	(1)(3)(7)
(3)3	59	15.21	(1)(2)
(4)4	1	41.5	
(5)5	11	50.86	
(6)6	1	80.1	
(7)7	14	10.91	(1)(2)
(8)8	25	25.51	(1)
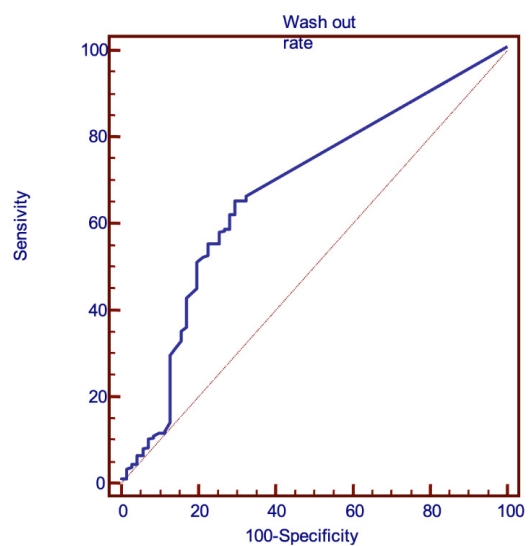
Graph 8. "Wash-out rate" ROC curve analysis

The "area under curve" and "wash-in" values of hemangioendothelioma and lymphomas are different from those of HCC, metastases, and hepatic adenoma (Graph 9).
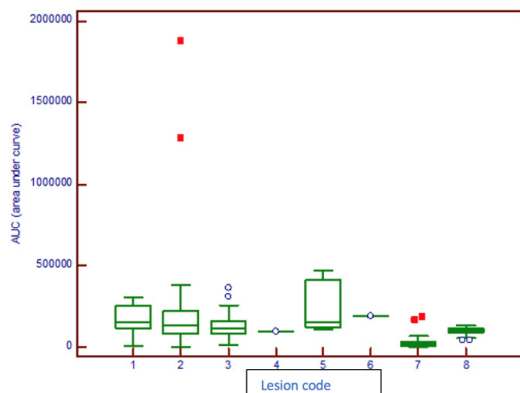
Graph 9. The distribution of the "AUC" values of the lesions (1 = HCC, 2 = Metastasis, 3 = Hemangioma, 4 = FNH, 5 = Adenoma, 6 = Angiomyolipoma, 7 = Hemangioendothelioma, 8 = Lymphoma)
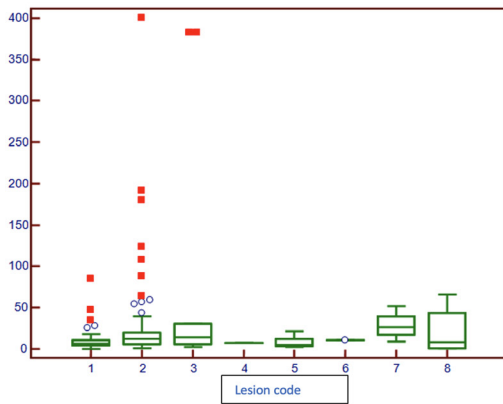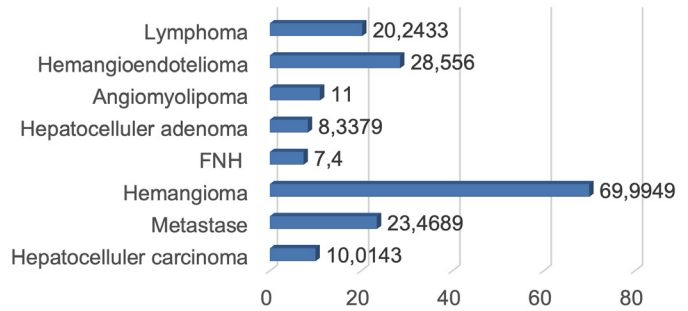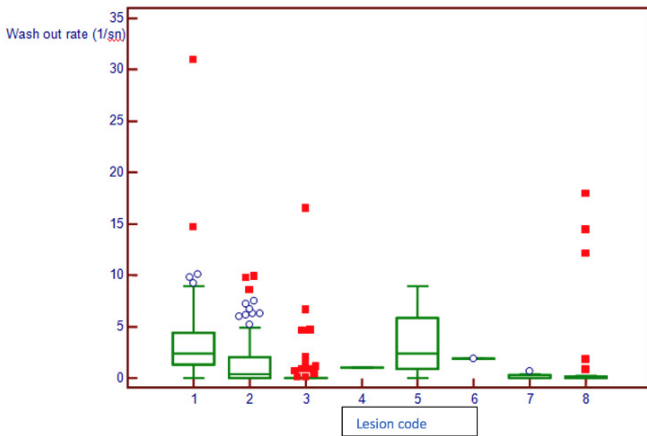

Graph 10. Distribution of lesions based on the type of curve (1 = HCC, 2 = Metastasis, 3 = Hemangioma, 4 = FNH, 5 = Adenoma, 6 = Angiomyolipoma, 7 = Hemangioendothelioma, 8 = Lymphoma)

TIC curve analysis

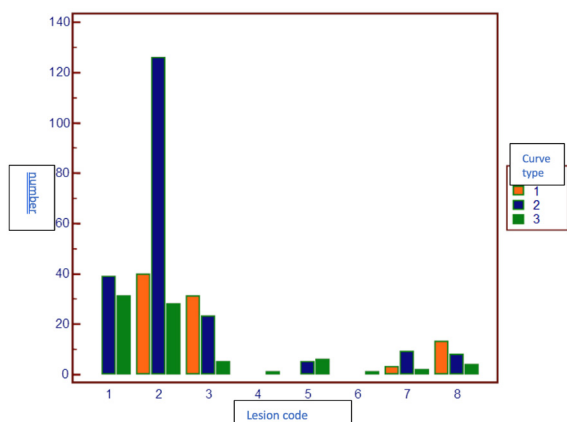The distribution of lesions according to curve types is shown in Graph 10. In our hemangioma cases, there were type I and type II curve patterns, predominantly type I. In hemangiomas over 2.5 cm, ROIs measured from the periphery of the lesion showed a type I curve almost completely. In hemangiomas and metastases, type I contrast enhancement curves were observed.

Contrast enhancement was present in the arterial phase in our HCC lesions. The type III contrast enhancement curve was observed in the majority (61.4%). All 27 lesions with a type II curve developed in a cirrhotic background, with 13 measuring less than 2 cm and 7 measuring more than 5 cm. In 12 lesions (>3 cm)

with a type II curve in ROI measurements including the whole lesion, a type III curve was observed in partial measurements.

Discussion

Accurate recognition and differentiation of FLL with noninvasive imaging techniques is important. Dynamic MRI can be used in clinical practice for noninvasive quantification of hepatic perfusion, which is essential in differential diagnosis.[9-11] The difference in changes in arterial and portal venous blood flow in benign and malignant lesions makes perfusion imaging complementary to conventional imaging in lesion detection and especially in characterization.[12] Perfusion MRI was first described for imaging regional and global blood flow in the heart, lung, and brain.[13] MR perfusion of the liver was reported in 1994 using gadolinium in rats.[14] Subsequently, several studies involving animal and human subjects were reported.[15] In the Materne study, tissue tracer concentration in rabbits was first estimated by empirical determination of the relationship between the pulse sequences used and the signal intensity and T1 values; then perfusion MR imaging was used to evaluate perfusion parameters in rabbits with and without cirrhosis and also in humans.[16,17] It has been suggested that perfusion imaging can be used as an in vivo marker of angiogenesis and even give more accurate results than histological examination, which is considered the gold standard for demonstrating angiogenesis.[18,19] Thanks to its high temporal and spatial resolution, DCE MRI increases the detectability of lesions even in less experienced observers. However, visual assessment of the wash-in and wash-out of lesions is sometimes difficult.[18] Therefore, it is advantageous to evaluate DCE MRI with functional maps and quantitative or semiquantitative parameters.[17,18] The goal of quantification techniques is to reduce the variability caused by the selection of imaging systems, magnetic field strengths, sequences, and parameters so that patients and centers can be compared. Kinetic parameters of quantification techniques may also contribute to the understanding of tumor biology.[12] Therefore, for applicability in daily practice, obtaining quantitative data should be simplified, reproducible, and less time-consuming. Our study demonstrated the applicability of semi-quantitative parameters derived from DCE-MRI functional maps in daily practice.

Mathematical modeling of imaging data is used to get quantitative measurement parameters like vascular density, permeability, perfusion, extravascular space, and plasma volume. These parameters are related to the pathophysiology of the lesion.[20] In a study comparing perfusion parameters between benign and malignant liver lesions, Ippolito et al. discovered that benign lesions had higher values than malignant ones (RAE 33.8

vs. 49.13%; RVE 66.03 vs. 40.54%; RLE 80.63 vs. 47.52%; ME 776 vs. 448.78%; MRE 86.27 vs. 49.85%; TTP 146.95 vs. 183.79%).[13] The usefulness of the perfusion and permeability parameters obtained in the detection of HCC and the differentiation of liver metastases and HCC has been reported.[21-23] The authors also reported that distribution volume and perfusion can distinguish liver metastases from neuroendocrine tumors according to their enhancement patterns (i.e., hypo- or hyper-rich).[24] Both arterial fraction and arterial hepatic blood flow have been shown to be significantly higher in HCC. Portal venous blood flow and volume of distribution have been found to be significantly lower in HCC compared to the surrounding cirrhotic parenchyma, possibly due to significant changes in tumor microvascular architecture and angiogenesis.[25] In the literature, it has been reported that quantitative parameters may also be useful in monitoring treatment response.[25, 26] Applications of quantitative MR perfusion have been investigated in the monitoring of treatment response after locoregional and systemic therapies in HCC.[27] Consistent with Taouli et al.[25] Ippolito et al. found differences in semi-quantitative perfusion analysis in tumors with and without completed TACE treatment.[26] The authors looked at how well perfusion MR imaging could show early changes after treatment. They found that those who were not targeted with TACE had significantly lower portal venous hepatic blood flow and a higher arterial fraction. In a study using rodents as a preclinical model, Braren et al. found that measuring the extravascular extracellular volume fraction one day after trans-arterial embolization was linked to more tumor necrosis.[28] In fact, Michielsen et al. reported the usefulness of perfusion parameters evaluated before TACE in predicting progression-free survival.[29] Hsu et al. showed that the Ktrans value was well correlated with tumor response, progression-free survival, and overall survival in patients receiving systemic therapy for advanced HCC and suggested that this may be related to changes in tumor vascularization caused by anti-angiogenic therapy.[30] Some studies have reported that early perfusion changes in advanced HCC are valuable in predicting overall survival after systemic therapy.[31,32] Similar results have been reported for K trans and various perfusion parameters in patients with colorectal metastases treated with chemotherapy in combination with targeted therapies. Coenegrachts et al. showed that the constant ratio between extravascular extracellular space and blood plasma (i.e., kep = Ktrans/ve) was significantly higher in treatment responders than in non-responders at baseline, with a significant decrease in this group after treatment.[33] De Bruyne et al. also associated a >40% reduction in Ktrans after treatment with longer progression-free survival.[34] Like Hirashima et al., Cannella et al. stated that changes can be seen in the early post-treatment period and observed chang-

es in both kep and Ktrans within one week after treatment, which may be helpful in predicting response to treatment.[6,35] But these quantitative data aren't very useful because they depend on a lot of different factors and take a lot of time to use.

Galbraith et al. reported that the use of complex pharmacokinetic modeling to generate fully quantitative parameters did not significantly alter the reproducibility of the technique and that simpler semiquantitative techniques were sufficiently reproducible in measuring relative changes in patients.[36] Some studies suggest that the semiquantitative DCE MRI perfusion parameters are different for hemangiomas and malignant tumors like HCC, cholangiocarcinoma, and metastases.[18,37]

In our study, the 0.08 threshold value we found for "wash-out" in DCE MR semiquantitative analysis is instructive in distinguishing between malignant and benign liver tumors. Ippolito et al. also reported that benign lesions showed higher values in semiquantitative analysis compared to malignant lesions, which is consistent with our findings.[38] It has also been reported that contrast enhancement and perfusion values in lesion groups may provide complementary quantitative information that may improve the final diagnostic accuracy if those with similar patterns can be clustered into subtypes. Therefore, we believe that the combination of functional information with morphological findings and research in larger case series with an increased number of subgroups for reproducible semiquantitative analysis may provide a standardized method that can be easily incorporated into the clinical workflow. Still, there will always be some variation because of changes in tissue blood flow, magnetic field changes, patient position, and body temperature.[18,39,40] In our study, the higher maximum relative enhancement of hemangiomas compared to metastases and the longer "wash-in" time of metastases compared to hemangiomas; the significantly shorter time between the arrival of contrast to the tissue and peak intensity time (TTP) in our HCC cases compared to metastases and hemangiomas; and the difference in BOE values in HCC, hemangiomas, and metastases (F ratio: 3.51, p=0.001) may be clues for the differential diagnosis. The difference may be explained by the fact that hemangiomas consist of blood-filled cavities lined with endothelium over a thin fibrous stroma and a large extracellular space, whereas malignant liver lesions show tumoral angiogenesis.[12,41] It has also been documented in the literature that HCCs are mainly supplied by the hepatic artery, whereas hypovascular metastases have a diffuse portal blood supply.[42] Abdullah et al. reported the usefulness of perfusion MRI in differentiating HCC and colorectal liver metastases.[43] DCE MRI arterial phase evaluation showed a positive predictive value of 82–90% and specificity of 80–99% for the diagnosis of hemangioma, HCC, and metastases.[18] In the literature,

the values of perfusion parameters (such as RAE, ME, and MRE) have been reported to be significantly higher in HCC lesions than in hypovascular metastases, consistent with the typical hypervascularity of HCC and the hypovascularity of metastases.[38] Although it is well documented that HCCs are mainly supplied by the hepatic artery and that hypovascular metastases have a diffuse portal blood supply[42], Alicioğlu et al. reported that no metric parameter could be identified to distinguish between HCCs and metastases.[18]

In metastases, differences may be observed depending on the degree of underlying hepatic arterial supply. However, there is some overlap between benign and malignant tumors. In this case, size may be effective; the lack of wash-in/wash-out phenomena in smaller tumors may be explained by the fact that angiogenesis has not yet developed. Another factor influencing behavior may be the degree of tumor cellular differentiation.[44] In our study, although the "wash in rate/wash out rate" value was higher in our haemangioma cases compared to metastasis and hepatocellular carcinoma (F ratio: 2.43, p<0.02), we could not obtain a reliable threshold value for discrimination in ROC curve analysis.

Although the number of lesions in our hemangioendothelioma and lymphoma cases was acceptable, the statistical data were homogenized because of the multiple lesions belonging to a small number of patients. However, a healthy interpretation can be made with the results of comprehensive analyses in subgroups.

Ippolito et al. and Donati et al. evaluated the diffusion and perfusion MRI features of FNH. They concluded that in semi-quantitative analysis, all lesions showed a rapid and marked increase followed by a rapid decay and then a slow decay, depending on the dominant arterial support, whereas the normal surrounding parenchyma showed a rapid increase followed by a plateau of slow decay; perfusion MRI may be an additional tool in accurately diagnosing FNH with the information it provides about the vascularity of the lesions.[38,45] It has been reported that functional-metric evaluation helps lesion characterization in the differentiation of hypervascular pseudolesions consisting of arterioportal shunts, which are frequently seen in cirrhosis or chronic hepatitis, and perilesional enhancement in metastatic lesions from true metastases.[18,46]

The degree of histopathological differentiation of the primary mass, as well as hypo- or hypervascularity, were found to be effective in observing a Type I contrast enhancement curve in metastases near hemangiomas in our study. However, since metastases were not classified in our study, no evaluation could be made in this direction. In future studies, the categorization of metastases considering the degree of vascularization and differentiation may help obtain meaningful clues for the differential diagnosis of the primary disease.

In clinical practice, quantification of hepatic blood flow has been reported for the assessment of liver metastases and chronic liver disease and for the study of the systemic availability of drugs.[9-11] Furthermore, hepatic perfusion parameters have been used to assess changes in sinusoidal permeability in cirrhosis.[15] The fact that all of the HCC lesions with a type II curve in our study developed on the background of chronic liver cirrhosis may be due to the limited specificity of arterial hypervascularity in cirrhotic livers, as well as inhomogeneity due to lesion size and poor sensitivity of portal and venous wash-out in lesions below 2 cm.[37] The observation of a type III curve in partial measurements in lesions >3 cm, which showed a type II curve in measurements including the whole lesion, suggested that partial measurements may be more sensitive due to the heterogeneity in the internal structure of HCC lesions with capsular staining. If the number of patients with HCC increases, the heterogeneity of the patient group and the variety of factors affecting the contrast kinetics of the lesion will increase, and the effects of the pattern difference in the curves due to mass, background liver, and measurement technique can be revealed in more detail.

Although diffusion-weighted (DW) MRI is widely used in clinical practice to differentiate focal liver lesions, it has been reported that quantitative ADC threshold values have variable accuracy depending on many factors, such as lesion type, b-values used for acquisition, and necrosis or fibrotic changes in malignant lesions, and that differentiation should not be made by ADC measurement alone due to the overlap of malignant and benign lesions and the differentiation of tumors.[47-49] Inclusion of parameters in algorithms will probably reduce the number of suspicious cases; however, in our study, we evaluated semiquantitative analysis data, not diffusion parameters.

Study limitations

Our study had some limitations. Firstly, although a large patient-lesion population was included in the study, statistical evaluation became impossible for some lesion types due to our limited number of cases. Secondly, the placement of ROIs by a single reader may be considered as a limitation. Thirdly, considering our cirrhotic patients, the surrounding liver used as reference tissue was not the same between the two groups. Furthermore, semiquantitative analysis may be affected by acquisition parameters, injection protocols, including contrast volume and injection rate, and physiological conditions such as respiratory movement.[50] Therefore, overlapping quantitative values of a single perfusion parameter may represent a bias in functional analysis, but multiparametric evaluations including conventional sequences and DWI may be the solution.

The current status of quantitative MRI in FLLs is somewhat paradoxical. Although numerous studies and clinics report promising results, their application in clinical practice is scarce. However, as seen in our study, quantitative data combined with qualitative imaging may provide solutions in various clinical situations. However, the clinical applications of perfusion imaging for FLLs are limited. The reasons for this include complex pharmacokinetic models caused by the fact that the liver is a mobile, blood-filled, flexible organ with double vascular access and fenestrated sinusoids, differences in imaging systems, non-standardized acquisition protocols, respiratory movements, possible iron overload, and starvation. This situation also makes it difficult to compare research studies. Most of the published studies are single-center and retrospective, and standardized acquisition parameters, post-procedural methods, or predicted results cannot be reported. The complex procedure required for perfusion quantification limits its use.[5,6] To overcome the limitations, the medical imaging community and the Alliance for Quantitative Imaging Biomarkers, the Radiological Society of North America, or the Biomarker Inventory are making a collective effort. The fact that new sequences, such as golden angle radial sparse parallel (GRASP) imaging, allow safe assessment of hepatic perfusion parameters with quantitative results comparable to perfusion CT, gives hope that next-generation sequences will make perfusion data more readily available.[51-53]

Conclusion

DCE MRI semiquantitative analysis of the abdomen may be useful in daily practice as a potential aid in differential diagnosis by providing noninvasive in vivo information about the nutrition and microvascular properties of lesions without increasing the application time. Furthermore, it may facilitate diagnostic studies in the detection and staging of hepatic diseases, treatment follow-up, and the development of anti-tumor drugs.

In our study, we thought that the difference in "Tpeak" and "wash-out" rate values in the semiquantitative analysis of DCE MR TIC in the differentiation of HCC, metastasis, and hemangioma and the 0.08 threshold value we found for "wash-out" in the ROC curve analysis in the differentiation of malignant and benign lesions of focal liver lesions may be guiding. Therefore, the comparison of semiquantitative analysis in larger case series in which the number of subgroups is increased may provide new opportunities as a reproducible, standardized method that can be easily combined with clinical workflow.

Declarations

Author contributions
Conceptualization, H.G.D. and Z.G.K.; Methodology, H.G.D and Z.G.K; Software, M.O.A.; Validation, H.G.D., D.A.U and N.K.; Formal Analysis, H.G.D.; Investigation, H.G.D. and D.A.U; Resources, H.G.D. and D.A.U.; Data Curation, H.G.D. and N.K; Writing – Original Draft Preparation, H.G.D. and D.A.U; Writing – Review & Editing, H.G.D., Z.G.K; Visualization, H.G.D. and M.O.A; Supervision, H.G.D. and Z.G.K.

Conflicts of interest
Authors state no conflict of interest.

Data availability
The datasets used and/or analyzed during the present study are available from the corresponding author upon reasonable request.

Ethics approval
This article does not contain any studies with human participants or animals performed by any of the authors. All data was processed anonymously, according to the privacy legislation.

References

1. Matos AP, Velloni F, Ramalho M, AlObaidy M, Rajapaksha A, Semelka RC. Focal liver lesions: Practical magnetic resonance imaging approach. *World J Hepatol.* 2015;7(16):1987-2008. doi: 10.4254/wjh.v7.i16.1987

2. Cogley JR, Miller FH. MR imaging of benign focal liver lesions. *Radiol Clin North Am.* 2014;52(4):657-682. doi: 10.1016/j.rcl.2014.02.005

3. Watanabe A, Ramalho M, AlObaidy M, Kim HJ, Velloni FG, Semelka RC. Magnetic resonance imaging of the cirrhotic liver: An update. *World J Hepatol.* 2015;7(3):468-487. doi: 10.4254/wjh.v7.i3.468

4. Belghiti J, Cauchy F, Paradis V, Vilgrain V. Diagnosis and management of solid benign liver lesions. *Nat Rev Gastroenterol Hepatol.* 2014;11(12):737-749. doi: 10.1038/nrgastro.2014.151

5. Ronot M, Lambert S, Daire JL, et al. Can we justify not doing liver perfusion imaging in 2013?. *Diagn Interv Imaging.* 2013;94(12):1323-1336. doi: 10.1016/j.diii.2013.06.005

6. Cannella R, Sartoris R, Grégory J, et al. Quantitative magnetic resonance imaging for focal liver lesions: bridging the gap between research and clinical practice. *Br J Radiol.* 2021;94(1122):20210220. doi: 10.1259/bjr.20210220

7. Hussain SM, Semelka RC. Hepatic imaging: comparison of modalities. *Radiol Clin North Am.* 2005;43(5):929-ix. doi: 10.1016/j.rcl.2005.05.006

8. Ronot M, Clift AK, Vilgrain V, Frilling A. Functional imaging in liver tumours. *J Hepatol.* 2016;65(5):1017-1030. doi: 10.1016/j.jhep.2016.06.024

9. Bader TR, Herneth AM, Blaicher W, et al. Hepatic perfusion after liver transplantation: noninvasive measurement with

dynamic single-section CT. *Radiology*. 1998;209(1):129-134. doi: 10.1148/radiology.209.1.9769823

10. Leggett DA, Kelley BB, Bunce IH, Miles KA. Colorectal cancer: diagnostic potential of CT measurements of hepatic perfusion and implications for contrast enhancement protocols. *Radiology*. 1997;205(3):716-720. doi: 10.1148/radiology.205.3.9393526

11. Van Beers BE, Leconte I, Materne R, Smith AM, Jamart J, Horsmans Y. Hepatic perfusion parameters in chronic liver disease: dynamic CT measurements correlated with disease severity. *AJR Am J Roentgenol*. 2001;176(3):667-673. doi: 10.2214/ajr.176.3.1760667

12. Nino-Murcia M, Olcott EW, Jeffrey RB Jr, Lamm RL, Beaulieu CF, Jain KA. Focal liver lesions: pattern-based classification scheme for enhancement at arterial phase CT. *Radiology*. 2000;215(3):746-751. doi: 10.1148/radiology.215.3.r00jn03746

13. Ippolito D, Colombo M, Trattenero C, et al. Diagnostic Value of Semiquantitative Analysis of Dynamic Susceptibility Contrast Magnetic Resonance Imaging with GD-EOB-DTPA in Focal Liver Lesions Characterization: A Feasibility Study. *Gastroenterol Res Pract*. 2015;2015:630273. doi: 10.1155/2015/630273

14. Reimer P, Saini S, Kwong KK, Cohen MS, Weissleder R, Brady TJ. Dynamic gadolinium-enhanced echo-planar MR imaging of the liver: effect of pulse sequence and dose on enhancement. *J Magn Reson Imaging*. 1994;4(3):331-335. doi: 10.1002/jmri.1880040318

15. Materne R, Smith AM, Peeters F, et al. Assessment of hepatic perfusion parameters with dynamic MRI. *Magn Reson Med*. 2002;47(1):135-142. doi: 10.1002/mrm.10045

16. Van Beers BE, Materne R, Annet L, et al. Capillarization of the sinusoids in liver fibrosis: noninvasive assessment with contrast-enhanced MRI in the rabbit. *Magn Reson Med*. 2003;49(4):692-699. doi: 10.1002/mrm.10420

17. Annet L, Materne R, Danse E, Jamart J, Horsmans Y, Van Beers BE. Hepatic flow parameters measured with MR imaging and Doppler US: correlations with degree of cirrhosis and portal hypertension. *Radiology*. 2003;229(2):409-414. doi: 10.1148/radiol.2292021128

18. Alicioglu B, Guler O, Bulakbasi N, Akpinar S, Tosun O, Comunoglu C. Utility of semiquantitative parameters to differentiate benign and malignant focal hepatic lesions. *Clin Imaging*. 2013;37(4):692-696. doi: 10.1016/j.clinimag.2013.01.012

19. Chandarana H, Taouli B. Diffusion and perfusion imaging of the liver. *Eur J Radiol*. 2010;76(3):348-358. doi: 10.1016/j.ejrad.2010.03.016

20. Koh DM, Padhani AR. Functional magnetic resonance imaging of the liver: parametric assessments beyond morphology. *Magn Reson Imaging Clin N Am*. 2010;18(3):565-xii. doi: 10.1016/j.mric.2010.07.002

21. Pahwa S, Liu H, Chen Y, et al. Quantitative perfusion imaging of neoplastic liver lesions: A multi-institution study. *Sci Rep*. 2018;8(1):4990. doi: 10.1038/s41598-018-20726-1

22. Ghodasara S, Pahwa S, Dastmalchian S, Gulani V, Chen Y. Free-Breathing 3D Liver Perfusion Quantification Using a Dual-Input Two-Compartment Model. *Sci Rep*. 2017;7(1):17502. doi: 10.1038/s41598-017-17753-9

23. Totman JJ, O'gorman RL, Kane PA, Karani JB. Comparison of the hepatic perfusion index measured with gadolinium-enhanced volumetric MRI in controls and in patients with colorectal cancer. *Br J Radiol*. 2005;78(926):105-109. doi: 10.1259/bjr/13525061

24. Koh TS, Thng CH, Hartono S, et al. Dynamic contrast-enhanced MRI of neuroendocrine hepatic metastases: A feasibility study using a dual-input two-compartment model. *Magn Reson Med*. 2011;65(1):250-260. doi: 10.1002/mrm.22596

25. Taouli B, Johnson RS, Hajdu CH, et al. Hepatocellular carcinoma: perfusion quantification with dynamic contrast-enhanced MRI. *AJR Am J Roentgenol*. 2013;201(4):795-800. doi: 10.2214/AJR.12.9798

26. Ippolito D, Trattenero C, Talei Franzesi C, et al. Dynamic Contrast-Enhanced Magnetic Resonance Imaging With Gadolinium Ethoxybenzyl Diethylenetriamine Pentaacetic Acid for Quantitative Assessment of Vascular Effects on Hepatocellular-Carcinoma Lesions Treated by Transarterial Chemoembolization or Radiofrequency Ablation. *J Comput Assist Tomogr*. 2016;40(5):692-700. doi: 10.1097/RCT.0000000000000427

27. Campos M, Candelária I, Papanikolaou N, et al. Perfusion Magnetic Resonance as a Biomarker for Sorafenib-Treated Advanced Hepatocellular Carcinoma: A Pilot Study. *GE Port J Gastroenterol*. 2019;26(4):260-267. doi: 10.1159/000493351

28. Braren R, Altomonte J, Settles M, et al. Validation of preclinical multiparametric imaging for prediction of necrosis in hepatocellular carcinoma after embolization. *J Hepatol*. 2011;55(5):1034-1040. doi: 10.1016/j.jhep.2011.01.049

29. Michielsen K, De Keyzer F, Verslype C, Dymarkowski S, van Malenstein H, Oyen R, Maleux G, et al. Pretreatment DCE-MRI for prediction of pfs in patients with inoperable HCC treated with TACE. *Cancer Imaging* 2011;11(1A):114. doi: 10.1102/1470-7330.2011.9058

30. Hsu CY, Shen YC, Yu CW, et al. Dynamic contrast-enhanced magnetic resonance imaging biomarkers predict survival and response in hepatocellular carcinoma patients treated with sorafenib and metronomic tegafur/uracil. *J Hepatol*. 2011;55(4):858-865. doi: 10.1016/j.jhep.2011.01.032

31. Kim KA, Park MS, Ji HJ, et al. Diffusion and perfusion MRI prediction of progression-free survival in patients with hepatocellular carcinoma treated with concurrent chemoradiotherapy. *J Magn Reson Imaging*. 2014;39(2):286-292. doi: 10.1002/jmri.24161

32. Chen BB, Hsu CY, Yu CW, et al. Early perfusion changes within 1 week of systemic treatment measured by dynamic contrast-enhanced MRI may predict survival in patients

with advanced hepatocellular carcinoma. *Eur Radiol*. 2017;27(7):3069-3079. doi: 10.1007/s00330-016-4670-2

33. Coenegrachts K, Bols A, Haspeslagh M, Rigauts H. Prediction and monitoring of treatment effect using T1-weighted dynamic contrast-enhanced magnetic resonance imaging in colorectal liver metastases: potential of whole tumour ROI and selective ROI analysis. *Eur J Radiol*. 2012;81(12):3870-3876. doi: 10.1016/j.ejrad.2012.07.022

34. De Bruyne S, Van Damme N, Smeets P, et al. Value of DCE-MRI and FDG-PET/CT in the prediction of response to preoperative chemotherapy with bevacizumab for colorectal liver metastases. *Br J Cancer*. 2012;106(12):1926-1933. doi: 10.1038/bjc.2012.184

35. Hirashima Y, Yamada Y, Tateishi U, et al. Pharmacokinetic parameters from 3-Tesla DCE-MRI as surrogate biomarkers of antitumor effects of bevacizumab plus FOLFIRI in colorectal cancer with liver metastasis. *Int J Cancer*. 2012;130(10):2359-2365. doi: 10.1002/ijc.26282

36. Galbraith SM, Lodge MA, Taylor NJ, et al. Reproducibility of dynamic contrast-enhanced MRI in human muscle and tumours: comparison of quantitative and semi-quantitative analysis. *NMR Biomed*. 2002;15(2):132-142. doi: 10.1002/nbm.731

37. Chen J, Si Y, Zhao K, et al. Evaluation of quantitative parameters of dynamic contrast-enhanced magnetic resonance imaging in qualitative diagnosis of hepatic masses. *BMC Med Imaging*. 2018;18(1):56. doi: 10.1186/s12880-018-0299-8

38. Ippolito D, Colombo M, Trattenero C, et al. Diagnostic Value of Semiquantitative Analysis of Dynamic Susceptibility Contrast Magnetic Resonance Imaging with GD-EOB-DTPA in Focal Liver Lesions Characterization: A Feasibility Study. *Gastroenterol Res Pract*. 2015;2015:630273. doi: 10.1155/2015/630273

39. Goh V, Padhani AR. Imaging tumor angiogenesis: functional assessment using MDCT or MRI?. *Abdom Imaging*. 2006;31(2):194-199. doi: 10.1007/s00261-005-0387-4

40. Leach MO, Brindle KM, Evelhoch JL, et al. Assessment of antiangiogenic and antivascular therapeutics using MRI: recommendations for appropriate methodology for clinical trials. *Br J Radiol*. 2003;76 Spec No 1:S87-S91. doi: 10.1259/bjr/15917261

41. Thng CH, Koh TS, Collins DJ, Koh DM. Perfusion magnetic resonance imaging of the liver. *World J Gastroenterol*. 2010;16(13):1598-1609. doi: 10.3748/wjg.v16.i13.1598

42. Materne R, Van Beers BE, Smith AM, et al. Non-invasive quantification of liver perfusion with dynamic computed tomography and a dual-input one-compartmental model. *Clin Sci (Lond)*. 2000;99(6):517-525.

43. Abdullah SS, Pialat JB, Wiart M, et al. Characterization of hepatocellular carcinoma and colorectal liver metastasis by means of perfusion MRI. *J Magn Reson Imaging*. 2008;28(2):390-395. doi: 10.1002/jmri.21429

44. Ito K. Hepatocellular carcinoma: conventional MRI findings including gadolinium-enhanced dynamic imaging. *Eur J Radiol*. 2006;58(2):186-199. doi: 10.1016/j.ejrad.2005.11.039

45. Donati F, Boraschi P, Gigoni R, Salemi S, Falaschi F, Bartolozzi C. Focal nodular hyperplasia of the liver: diffusion and perfusion MRI characteristics. *Magn Reson Imaging*. 2013;31(1):10-16. doi: 10.1016/j.mri.2012.06.031

46. Yu JS, Rofsky NM. Hepatic metastases: perilesional enhancement on dynamic MRI. *AJR Am J Roentgenol*. 2006;186(4):1051-1058. doi: 10.2214/AJR.04.169

47. Taouli B. Diffusion-weighted MR, imaging for liver lesion characterization: a critical look. *Radiology*. 2012;262:378-380.

48. Soyer P, Corno L, Boudiaf M, et al. Differentiation between cavernous hemangiomas and untreated malignant neoplasms of the liver with free-breathing diffusion-weighted MR imaging: comparison with T2-weighted fast spin-echo MR imaging. *Eur J Radiol*. 2011;80:316–24.

49. Wagner M, Doblas S, Daire JL, et al. Diffusion-weighted MR imaging for the regional characterization of liver tumors. *Radiology*. 2012;264:464-472.

50. Donato H, França M, Candelária I, Caseiro-Alves F. Liver MRI: From basic protocol to advanced techniques. *Eur J Radiol*. 2017;93:30-39. doi: 10.1016/j.ejrad.2017.05.028

51. Quantitative Imaging Biomarkers Alliance. 2021. Available from: https://www.rsna. org/en/research/quantitative-imaging- biomarkers-alliance. Accessed February 1, 2021.

52. Biomarker Inventory. Available from: https://www.myesr.org/research/biomarkers-inventory. Accessed February 1, 2021.

53. Weiss J, Ruff C, Grosse U, Grözinger G, Horger M, Nikolaou K, et al. Assessment of hepatic perfusion using GRASP MRI: bringing liver MRI on a new level. *Invest Radiol*. 2019; 54:737-743. doi: 10.1097/RLI.0000000000000586